

[Home](#)[About us](#)

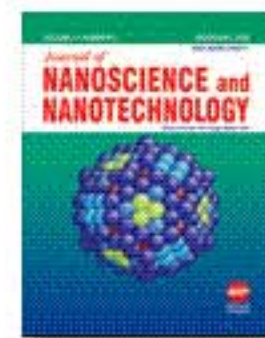
[Advanced search](#)Browse by: [Publication](#) [Publisher](#) [Subject](#)[Home](#) >> [Journal of Nanoscience and Nanotechnology](#), Volume 12, Number 4

S Effect of Curing Temperature on Nano-Silver Paste Ink for Organic Thin-Film Transistors

Authors: Kim, Minseok; Koo, Jae Bon; Baeg, Kang-Jun; Noh, Yong-Young; Yang, Yong Suk; Jung, Soon-Won; Ju, Byeong-Kwon; You, In-Kyu

Source: [Journal of Nanoscience and Nanotechnology](#), Volume 12, Number 4, April 2012, pp. 3272-3275(4)

Publisher: [American Scientific Publishers](#)



[< previous article](#) | [view table of contents](#) | [next article >](#)

S You have access to the full text electronic article

You, or the institution you are accessing from, have subscription access to this publication.

View now:

 1,073.2kb
Abstract:

Silver (Ag) metal electrode having 20 μm channel length was printed by reverse offset printing (ROP) using nano-silver paste ink for the source/drain of organic thin-film transistors (OTFT). Specific resistance and surface roughness of printed Ag electrodes with increasing curing temperature were investigated, and surface morphology and grain growth mechanism were systematically verified using a scanning electron microscope (SEM) and atomic force microscope (AFM) in order to obtain an optimized ROP Ag electrode. The Ag electrode was applied to fabricate top-gate/bottom-contact poly(3-hexylthiophene) OTFT devices, which showed reproducible OTFT characteristics such as the field-effect mobility, threshold voltage, and an on/off-current ratio of $\sim 10^{-3} \text{ cm}^2/\text{Vs}$, 0.36 V, and $\sim 10^2$, respectively.

[Articles that cite this article?](#)

Document Type: Research Article

DOI: <http://dx.doi.org/10.1166/inn.2012.5639>

Publication date: 2012년 4월 1일 (일)

[> More about this publication?](#)

[> Related content](#)

You are signed in as:

Korea University

(Institutional account)

KESLI Brill Consortium

(Institutional account)

kesli2006

(Institutional account)

[Additional sign in](#) | [Sign out](#)

[Marked list](#)**Tools**


[Activate personal subscription](#)

+ [Export options](#)

+ [Linking options](#)

 [Receive new issue alert](#)

 [Latest TOC RSS Feed](#)

 [Recent Issues RSS Feed](#)

 [Get Permissions](#)

Key

F Free content

N New content

OA Open access content

S Subscribed content

T Free trial content

Text size:

[a](#) | [a](#) | [a](#) | [a](#)

Effect of Curing Temperature on Nano-Silver Paste Ink for Organic Thin-Film Transistors

Minseok Kim^{1,2}, Jae Bon Koo^{1,*}, Kang-Jun Baeg¹, Yong-Young Noh³, Yong Suk Yang¹,
Soon-Won Jung¹, Byeong-Kwon Ju^{2,*}, and In-Kyu You¹

¹Convergence Components and Materials Research Laboratory, Electronics and Telecommunications
Research Institute, Daejeon 305-700, Korea

²Display and Nanosystem Laboratory, College of Engineering, Korea University, Seoul 136-713, Korea

³Department of Chemical Engineering, Hanbat National University, Daejeon 305-719, Korea

Silver (Ag) metal electrode having 20 μm channel length was printed by reverse offset printing (ROP) using nano-silver paste ink for the source/drain of organic thin-film transistors (OTFT). Specific resistance and surface roughness of printed Ag electrodes with increasing curing temperature were investigated, and surface morphology and grain growth mechanism were systematically verified using a scanning electron microscope (SEM) and atomic force microscope (AFM) in order to obtain an optimized ROP Ag electrode. The Ag electrode was applied to fabricate top-gate/bottom-contact poly(3-hexylthiophene) OTFT devices, which showed reproducible OTFT characteristics such as the field-effect mobility, threshold voltage, and an on/off-current ratio of $\sim 10^{-3}$ cm^2/Vs , 0.36 V, and $\sim 10^2$, respectively.

Keywords: Curing Temperature, Nano-Silver Paste, OTFT, Reverse Offset Printing.

IP: 163.152.52.92 On: Wed, 19 Mar 2014 01:38:02

Copyright: American Scientific Publishers

1. INTRODUCTION

The field of organic electronics has been widely studied by many researchers wanting to develop a variety of high performance and/or high resolution organic opto/electronic devices, such as organic light-emitting diodes (OLEDs),¹ organic field-effect transistors (OFETs),^{2,3} organic photovoltaics (OPVs),⁴ organic non-volatile memory,⁵ and bio-/chemical-sensors.⁶ Various graphic art printing techniques, such as gravure, inkjet, and reverse offset printing (ROP) have been shown to make it possible to realize flexible, large-area, and low-cost organic opto/electronic devices and circuits. For instance, Baeg et al. developed high speed complementary polymer circuits of ~ 50 kHz switching speeds based on the inkjet-printing process;⁷ however, they used conventional photolithographic metal electrode processing for fabrication of the organic thin-film transistors (OTFTs).

The mass-production printing methods, such as gravure and ROP, are substantially notable for largely enhanced productivity and throughput in comparison with other printing methods.⁸ However, printing resolution and surface morphologies of the printed patterns via mass-production roll-to-roll (R2R) processes have limited the

application area of such printing processes. State-of-the-art printing resolution is in the range of 20 μm for ROP and gravure printing, with 1 μm below film thickness. It is well known that the improvement of charge carrier mobility and the downscaling of channel length (L) are essential in order to increase switching speeds of OTFTs and their integrated circuits.⁹ Gravure printing, however, has typically been limited to very low device performance because of its poor line resolution and registration.

In this study, therefore, the ROP technique was used for fabrication of OTFTs. It should be noted that this printing method is very attractive because of a variety of advantages, such as very high resolution (potentially available up to below 1 μm) and high throughput, no limitation to substrate types or sizes, and ability to print very tiny and various shaped patterns. Surface morphology and electrical properties of the printed nano-silver paste ink after changing the post thermal annealing process were systematically investigated. Optimized Ag printed patterns were utilized to fabricate top-gate/bottom-contact polymer transistors that showed reproducible and acceptable OTFT characteristics.

2. EXPERIMENTAL DETAILS

An Ag electrode having 20 μm channel length was fabricated using a sheet-to-sheet reverse offset printer (Narae

*Authors to whom correspondence should be addressed.

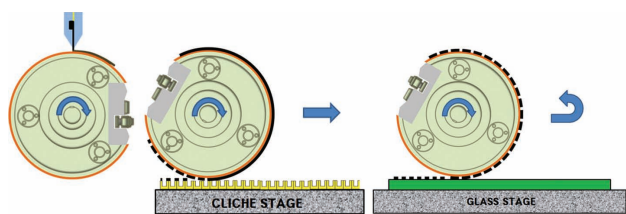


Fig. 1. Schematic illustration of the plate to plate reverse offset printing process.

NanoTech Corporation). The nano-silver paste ink (DGH ink, Advanced Nano Products Co., LTD.) (39 wt%) with 1.5 cPs of viscosity and 25.8 mN/m of surface tension was dispensed on the surface of the blanket roll (PDMS type, KNW) by controlling the syringe pump. While the blanket rolled on cliché with 20 μm patterns at 15 mm/s speed, unnecessary ink was removed from the blanket and was transferred to the top of the cliché surface. The remained ink for the desired pattern on the blanket was transferred onto the 160 \times 160 mm glass substrates at room temperature (Fig. 1). Post thermal treatment was individually carried out in the furnace at temperatures ranging from 150 to 450 $^{\circ}\text{C}$ with 50 $^{\circ}\text{C}$ steps for 30 minutes in order to remove the various additives and residual solvent in the printed Ag ink. The sheet resistance and thickness of the printed Ag patterns were measured at about five different points. The crystal structure and the surface morphology of the printed Ag ink were analyzed using a scanning electron microscope (SEM) and atomic force microscope (AFM) in order to optimize curing temperature of the metal electrodes. The poly(3-hexylthiophene) (P3HT) semiconducting polymer was dissolved in *p*-xylene (10 mg/ml), and poly(methyl methacrylate) (PMMA) gate dielectric material was dissolved in *n*-butyl acetate (80 mg/ml) at 80 $^{\circ}\text{C}$ for more than two hours. These solutions were subsequently spin-coated upon the printed Ag electrode. Finally, the Al gate electrode (100 nm) was deposited by thermal evaporator. *I*-*V* characteristics of the OTFT were measured using a KEITHLEY 4200-SCS in the dark in air.

3. RESULTS AND DISCUSSION

Figure 2 shows an optical microscope image of the printed source/drain (*S/D*) electrodes fabricated by ROP; these electrodes had a channel length of 20 μm . The thickness of the printed Ag electrodes was about 400 ± 20 nm. High resolution electrode patterns, with $L = 20$ μm and $W = 80$ μm , were typically obtained; individual OTFT were treated post annealing at 150, 200, 250, 300, 350, 400 and 450 $^{\circ}\text{C}$, each for 30 min.

The specific resistance, which was calculated from the thickness and the sheet resistance of the printed Ag pattern, was found to decrease rapidly with the increasing of the curing temperatures until 350 $^{\circ}\text{C}$; thereafter it increased slightly above the critical point (Fig. 3(a)). The value of

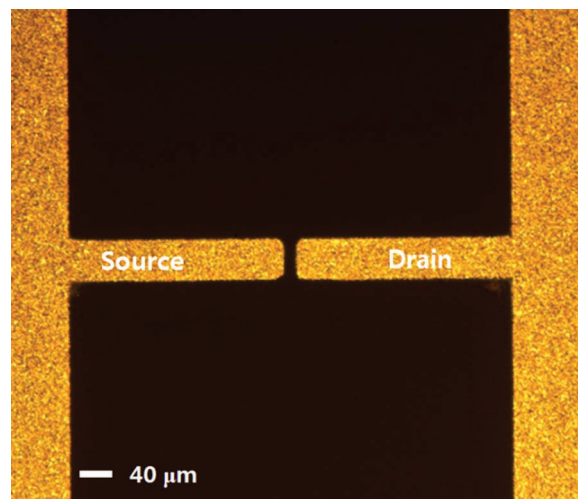


Fig. 2. Optical microscope image of the source and drain electrode made by reverse offset printing.

the specific resistance of the printed Ag ink was ca. 1.0×10^{-5} $\text{ohm} \cdot \text{cm}$ at 150 $^{\circ}\text{C}$, but rapidly dropped to 2.8×10^{-6} $\text{ohm} \cdot \text{cm}$ at 350 $^{\circ}\text{C}$ and increased to 4.5×10^{-6} $\text{ohm} \cdot \text{cm}$ at temperatures above 350 $^{\circ}\text{C}$. The decreased specific resistance with increasing curing temperature was mainly attributed to the growth of Ag grains and to the complete removal of the various additives and residual solvent in the printed Ag patterns. However, the specific resistance was not further reduced with the increased curing temperature above the critical annealing point (350 $^{\circ}\text{C}$). This can be explained by considering the SEM surface images of the printed Ag ink for curing temperature, as shown in Figure 3(b). It can be clearly observed that the grain size increased gradually with the increased curing temperature. This expansion is in good agreement with the experimental results shown in Figure 3(a). The initial crystal components of the nano-silver paste ink were found to impinge on each other in the two-dimensional orientation and their placement led them to adhere and form the crystal. Finally, the crystal structure grew as a whole, including in the three-dimensional orientation. Beyond the driving force that level of supersaturation, and discontinuous and cracked surface were found to occur, as shown in the inserted SEM images, at more than 400 $^{\circ}\text{C}$. These defects, such as the discontinuous and rough surface, are likely to bring a decrease in conductance of the printed Ag ink. In this regard, we can find that surface morphology was rapidly getting rough over 350 $^{\circ}\text{C}$, as shown in Figures 4(a and b). Figure 4 shows the surface roughness and the AFM morphology of the printed Ag ink. The root mean square roughness (R_{rms}) tends to increase, accompanying the grain growth from 150 to 450 $^{\circ}\text{C}$, but the R_{rms} was significantly increased from 29.1 nm at 350 $^{\circ}\text{C}$ to 72.0 nm at 450 $^{\circ}\text{C}$.

The OTFT with reverse-offset-printed *S/D* electrodes was fabricated, of which the $L = 20$ μm , $W = 80$ μm and thickness = 400 ± 20 nm (Fig. 5). In our experiment,

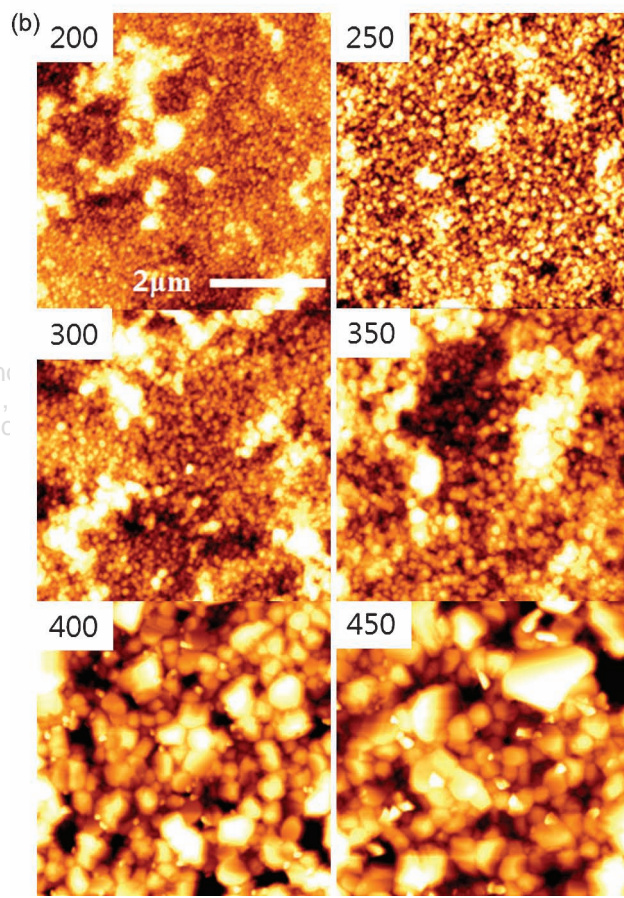
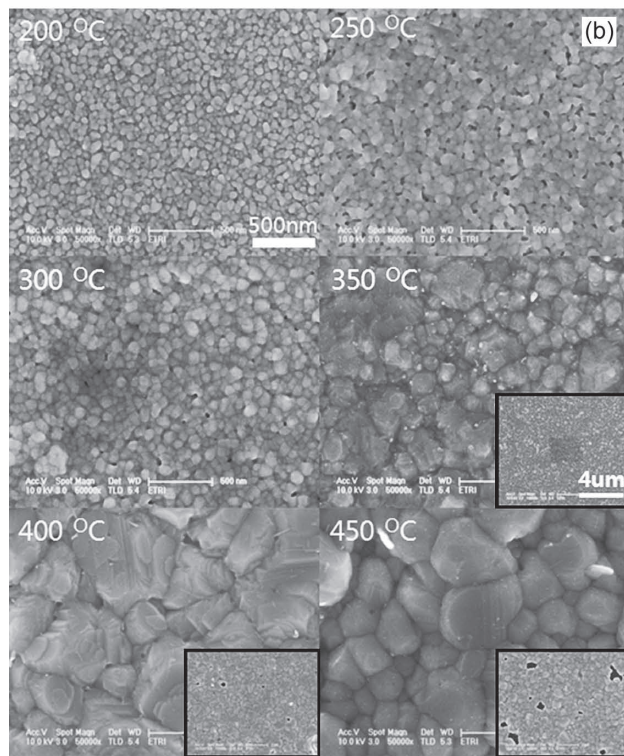
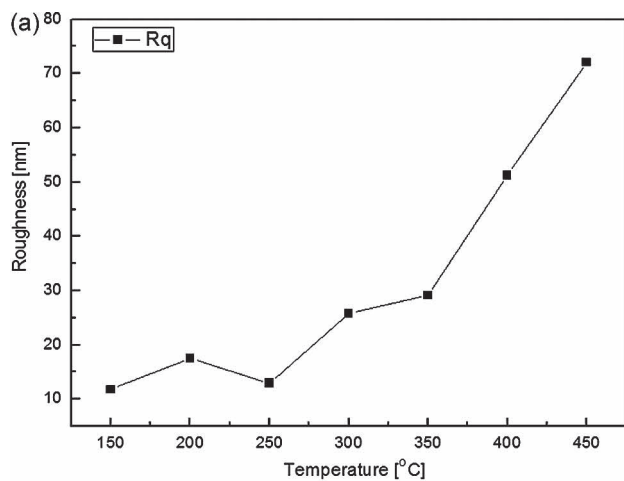
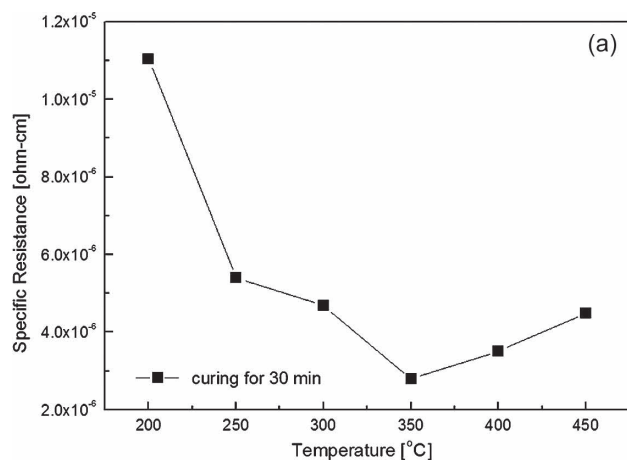


Fig. 3. (a) Specific resistance and (b) corresponding scanning electron microscope images of the printed nano-silver paste after each thermal annealing process.

Fig. 4. (a) Root mean square roughness and (b) corresponding surface morphologies, measured by atomic force microscope of the printed source and drain electrode.

in order to fully cover the relatively thick and rough source/drain electrodes, a thick active layer and insulator, as much as electrodes, was necessary for the top-gate/bottom-contact transistors. Because a smooth surface of the printed electrode is desirable for the high performance of the OTFT device, continuous active layers were deposited on top of the Ag patterns. For the active layer, the P3HT, which has ionization potential of -4.9 eV, was used as a polymer semiconductor.¹⁰ As insulator film, PMMA, with more than 500 nm thickness ($C_i = 6.2$ nF/cm²), was spin-coated onto the active layer. The Al was deposited by thermal evaporator on the top layer as a top gate metal. The transfer and output characteristics of these

OTFT are shown in Figures 6(a and b). The calculated field-effect mobility of the OTFT in the saturation region was ca. 3×10^{-3} cm²/Vs. It should be noted that the maximum mobility of the P3HT OTFT device was more than 1×10^{-1} cm²/Vs when measured in the inert atmosphere on a photolithography patterned gold source/drain electrode.⁷ Although the mobility is relatively lower than that of the top-gate reference devices, it is still comparable

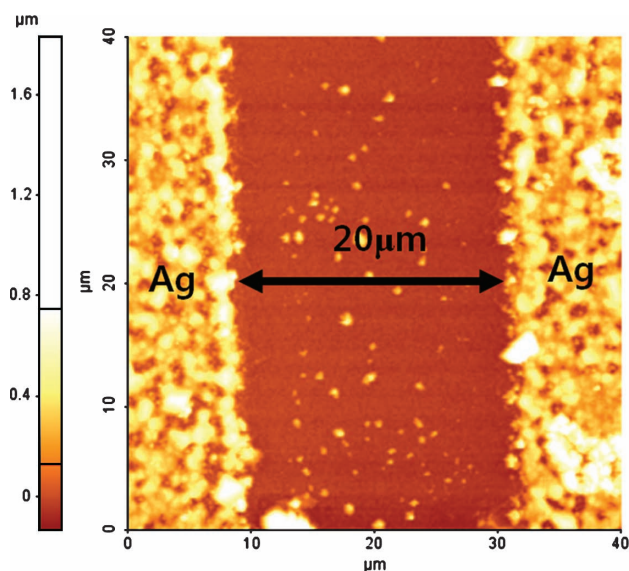


Fig. 5. Atomic force microscope image of the printed Ag source and drain electrodes made by reverse offset printing.

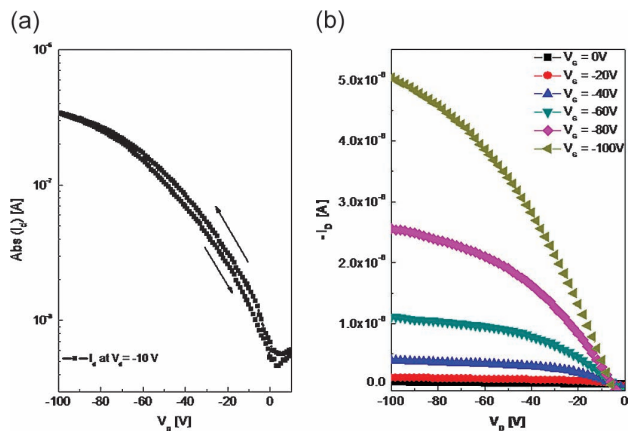


Fig. 6. (a) Transfer and (b) output characteristics of OTFT with printed source and drain electrodes.

to most of the typical bottom-gate P3HT OTFTs, as well as those made by using the Ag electrode. The threshold voltage and the on/off-current ratios were 0.36 V and under 10^2 , respectively. This relatively low on/off ratio can be attributed to the spin-coated P3HT active layer (un-patterned) and to the measurement in air, because the semi-conducting polymer P3HT has low oxidation stability.¹¹ Because of the work-function mismatch between Ag (-4.2 eV) and the highest occupied molecular orbital (HOMO) of *p*-type polymer semiconductor (-4.9 eV),¹⁰ we believe that the relatively low field-effect mobility of the printed Ag source/drain transistors presumably resulted from the contact resistance. Also, the rough surface and some of the large peaks of printed electrode led

to relatively high gate leakage current because of defects between the active layer and the gate insulator. This is a common problem for many printed electrode materials. Research into reducing contact resistance and gate leakage current, and thereby optimizing the OTFT performance, is currently under-way. We expect that high resolution and high throughput roll-to-roll printable Ag metal electrodes can be utilized in a variety of printed electronic applications, such as printed RFID tags,¹² TFT-backplanes for active matrix LCD and OLED¹⁻³ displays, and platforms of bio- and optical-sensors.⁶

4. CONCLUSION

We have demonstrated printed Ag source/drain with 20 μm short channel length by reverse offset printing, and investigated the effect of curing temperature on nano-silver paste ink for transistor electrodes. Reproducible and acceptable characteristics of top-gate OTFTs were achieved. But the printing process yields surface roughness and too thick of an electrode, etc., and many other problems remain.

Acknowledgments: This study was supported by the Development of New Materials and Solution Process for LCD Backplanes funded by ISTK (B551179-09-06-00), Basic Science Research Program, through the National Research Foundation of Korea (NRF), funded by the Ministry of Education, Science and Technology (2010-0015035) and by the Development of printing ink for touch panels and OLED lighting (A2010D-D006), funded by the Ministry of Knowledge Economy (MKE) and Daedeok innopolis.

References and Notes

1. D. J. Gundlach, *Nat. Mater.* 6, 173 (2007).
2. H. Klauk, *Nat. Mater.* 6, 397 (2007).
3. Y.-Y. Noh, N. Zhao, M. Caironi, and H. Sirringhaus, *Nat. Nanotechnol.* 2, 784 (2007).
4. S. R. Forrest, *Nature* 428, 911 (2004).
5. K.-J. Baeg, Y.-Y. Noh, J. Ghim, B. Lim, and D.-Y. Kim, *Adv. Funct. Mater.* 18, 3678 (2008).
6. B. Crone, A. Dodabalapur, A. Gelperin, L. Torsi, H. E. Katz, A. J. Lovinger, and Z. Bao, *Appl. Phys. Lett.* 78, 15 (2001).
7. K.-J. Baeg, D. Khim, D.-Y. Kim, S.-Y. Jung, J. B. Koo, I.-K. You, H. Yan, A. Facchetti, and Y.-Y. Noh, *J. Polymer Science Part B* 49, 62 (2011).
8. J. R. Sheats, *J. Mater. Research* 19, 1974 (2004).
9. M. Marinkovic, E. Hashem, K.-Y. Chan, A. Gordijn, H. Stiebig, and D. Knipp, *Appl. Phys. Lett.* 7, 97 (2010).
10. H. Sirringhaus, *Adv. Mater.* 17, 2411 (2005).
11. J. Ficker, H. von Seggern, H. Rost, W. Fix, W. Clemens, and I. McCulloch, *Appl. Phys. Lett.* 85, 1377 (2004).
12. P. F. Baude, D. A. Ender, M. A. Haase, T. W. Kelley, D. V. Muires, and S. D. Theiss, *Appl. Phys. Lett.* 82, 3964 (2003).

Received: 31 October 2010. Accepted: 5 February 2011.